

## Possibilities of finite calculus in computational mechanics

Eugenio Oñate<sup>\*,†</sup>

*International Center for Numerical Methods in Engineering (CIMNE), Universidad Politécnica de Cataluña,  
Edificio C1, Gran Capitán s/n, 08034, Barcelona, Spain*

### SUMMARY

The expression ‘finite calculus’ refers to the derivation of the governing differential equations in mechanics by invoking balance of fluxes, forces, etc. in a space–time domain of finite size. The governing equations resulting from this approach are different from those of infinitesimal calculus theory and they incorporate new terms which depend on the dimensions of the balance domain. The new governing equations allow the derivation of naturally stabilized numerical schemes using any discretization procedure. The paper discusses the possibilities of the finite calculus method for the finite element solution of convection–diffusion problems with sharp gradients, incompressible fluid flow and incompressible solid mechanics problems and strain localization situations. Copyright © 2004 John Wiley & Sons, Ltd.

**KEY WORDS:** finite calculus; computational mechanics; stabilized methods; finite element method; incompressible flow; incompressible solids; strain localization

### 1. INTRODUCTION

It is well known that standard numerical methods such as the central finite difference (FD) method, the Galerkin finite element (FE) method and the finite volume (FV) method, among others, lead to unstable numerical solutions when applied to problems involving different scales, multiple constraints and/or high gradients. Examples of these situations are typical in the solution of convection–diffusion problems, incompressible problems in fluid and solid mechanics and strain or strain rate localization problems in solids and compressible fluids using the standard Galerkin FE method or central scheme in FD and FV methods [1, 2]. Similar instabilities are found in the application of meshless methods to those problems [3–5].

The sources of the numerical instabilities in FE, FD and FV methods, for instance, have been sought in the apparent inability of the Galerkin FE method and the analogous central difference scheme in FD and FV methods, to provide a numerical procedure able to capture the different scales appearing in the solution for all ranges of the physical parameters. Typical examples

---

\*Correspondence to: Eugenio Oñate, International Center for Numerical Methods in Engineering (CIMNE), Universidad Politécnica de Cataluña, Edificio C1, Gran Capitán s/n, 08034 Barcelona, Spain.

†E-mail: onate@cimne.upc.es

are the spurious numerical oscillations in convection–diffusion problems for high values of the convective terms. The same type of oscillations are found in regions next to sharp internal layers appearing in high speed compressible flows (shocks) or in strain localization problems (shear bands) in solids. A similar problem of different nature emerges in the solution of incompressible problems in fluid and solid mechanics. Here the difficulties in satisfying the incompressibility constraint limit the choices of the approximation for the velocity (or displacement) variables and the pressure [1].

The solution of above problems has been attempted in a number of ways. The underdiffusive character of the central difference scheme for treating advective–diffusive problems has been corrected in an *ad hoc* manner by adding the so-called ‘artificial diffusion’ terms to the standard governing equation [2]. The same idea has been successfully applied to derive stabilized FV and FE methods for convection–diffusion and fluid-flow problems [1, 2]. Other stabilized FD schemes are based on the ‘upwind’ computation of the first derivatives appearing in the convective operator [2]. The counterpart of upwind techniques in the FEM are the so-called Petrov–Galerkin methods [1, 6], or the more general Galerkin methods [7] based on *ad hoc* residual-based extensions of the Galerkin variational form with the aim of achieving a stabilized numerical scheme. Among the many methods of this kind we can name the SUPG method [8–10], the Galerkin least square (GLS) method [11, 12], the characteristic Galerkin method [13–15], the characteristic based split (CBS) method [16, 17] and the subgrid scale (SS) method [18–21].

In this paper, we propose a different route to derive stabilized numerical methods. The starting point are the modified governing differential equations of the problem derived using a finite calculus (FIC) approach [22]. The FIC method is based in expressing the balance of fluxes (or equilibrium of forces) in a space–time domain of finite size. This introduces naturally additional terms in the classical differential equations of the infinitesimal theory which are a function of the balance domain dimensions. The merit of the modified equations via the FIC approach is that they lead to stabilized schemes using *any* numerical method. In addition, the different stabilized FD, FE and FV methods typically used in practice can be *recovered* using the FIC equations [22, 23]. Moreover, these equations are the basis for deriving a consistent procedure for computing the stabilization parameters [24, 25].

The layout of the paper is the following. In the next section the main concepts of the FIC method are introduced. Applications of the FIC method to convection–diffusion problems with sharp gradients are detailed and some examples of application are given. Finally, the possibilities of the FIC method in incompressible fluid and solid mechanics are discussed and a finite element formulation is presented. Next, the possibilities of the FIC method for strain localization problems in solids are briefly discussed.

## 2. THE FINITE CALCULUS METHOD

We will consider a convection–diffusion problem in a 1D domain  $\Omega$  of length  $L$ . The equation of balance of fluxes in a subdomain of size  $d$  belonging to  $\Omega$  (Figure 1) is written as

$$q_A - q_B = 0 \quad (1)$$

where  $q_A$  and  $q_B$  are the incoming and outgoing fluxes at points  $A$  and  $B$ , respectively. The flux  $q$  includes both convective and diffusive terms; i.e.  $q = v\phi - k(d\phi/dx)$ , where  $\phi$  is the

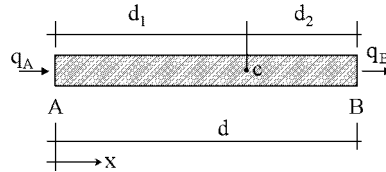


Figure 1. Equilibrium of fluxes in a space balance domain of finite size.

transported variable (i.e. the temperature in a thermal problem),  $v$  is the velocity and  $k$  is the diffusivity of the material.

Let us express now the fluxes  $q_A$  and  $q_B$  in terms of the flux at an arbitrary point  $C$  within the balance domain (Figure 1). Expanding  $q_A$  and  $q_B$  in Taylor series around point  $C$  up to second-order terms gives

$$q_A = q_C - d_1 \left. \frac{dq}{dx} \right|_C + \frac{d_1^2}{2} \left. \frac{d^2q}{dx^2} \right|_C + O(d_1^3), \quad q_B = q_C + d_2 \left. \frac{dq}{dx} \right|_C + \frac{d_2^2}{2} \left. \frac{d^2q}{dx^2} \right|_C + O(d_2^3) \quad (2)$$

Substituting Equation (2) into Equation (1) gives after simplification

$$\frac{dq}{dx} + \frac{h}{2} \frac{d^2q}{dx^2} = 0 \quad (3)$$

where  $h = d_1 - d_2$  and all the derivatives are computed at the arbitrary point  $C$ .

Standard calculus theory assumes that the domain  $d$  is of infinitesimal size and the resulting balance equation is simply  $dq/dx = 0$ . We will relax this assumption and allow the space balance domain to have a *finite size*. The new balance equation (3) incorporates now the underlined term which introduces the *characteristic length*  $h$ . Obviously, accounting for higher-order terms in Equation (2) does not change the balance equation (3) resulting in the parameter of  $h$ .

Distance  $h$  in Equation (3) can be interpreted as a free parameter depending on the location of point  $C$  within the balance domain. Note that  $-d \leq h \leq d$  and, hence,  $h$  can take a negative value. At the discrete solution level the domain  $d$  should be replaced by the balance domain around a node. This gives for an equal size discretization  $-l^e \leq h \leq l^e$  where  $l^e$  is the element or cell dimension. The fact that Equation (3) is the *exact balance equation* (up to second-order terms) for any 1D domain of finite size and that the position of point  $C$  is arbitrary, can be used to derive numerical schemes with enhanced properties simply by computing the characteristic length parameter from an adequate ‘optimality’ rule leading to a smaller error in the numerical solution [22–24].

Consider, for instance, Equation (3) applied to the 1D convection–diffusion problem. Neglecting third-order derivatives of  $\phi$ , Equation (3) can be rewritten in terms of  $\phi$  as

$$-v \frac{d\phi}{dx} + \left( k + \frac{vh}{2} \right) \frac{d^2\phi}{dx^2} = 0 \quad (4)$$

We see clearly that the FIC method introduces *naturally* an additional diffusion term in the standard convection–diffusion equation. This is the basis of the popular ‘artificial diffusion’ procedure [1, 2, 6] where the characteristic length  $h$  is typically expressed as a function of

the cell or element dimension. The *critical* value of  $h$  can be computed by introducing an optimality condition, such as obtaining a physically meaningful solution (such as  $\phi_i \geq 0$  for the Dirichlet problem with non-negative prescribed values of  $\phi$  at  $x = 0$  and  $x = L$ ). For an equal size discretization this gives  $h \geq (1 - 1/\gamma)l^e$ , where  $\gamma = vl^e/2k$  is the element/cell Peclet number [1]. Note that the inequality applies for  $\gamma > 0$  and it should be reversed for  $\gamma < 0$ . Also  $h = 0$  for  $|\gamma| < 1$  [22, 23]. Indeed an *optimal* value of  $h$  leading to exact nodal values can also be found for this simple case as  $h = (\coth \gamma - 1/\gamma)l^e$  [1].

The FIC method has been classified in Reference [26] as a particular case of ‘modified equations methods’ where the standard differential equations are first augmented using physical concepts and then discretized using any numerical technique. An interpretation of the FIC equations as a modified residual method is presented in Reference [27].

Equation (3) can be extended to account for source terms. The modified governing equation can then be written in compact form as

$$r - \frac{h}{2} \frac{dr}{dx} = 0 \quad (5)$$

with

$$r := -v \frac{d\phi}{dx} + \frac{d}{dx} \left( k \frac{d\phi}{dx} \right) + Q \quad (6)$$

where  $Q$  is the external source. For consistency a ‘finite’ form of the Neumann boundary condition should be used. This can be readily obtained by invoking balance of fluxes in a domain of finite size next to the boundary  $\Gamma_q$  where the external (diffusive) flux is prescribed to a value  $q_p$ . The modified Neumann boundary condition is [22]

$$k \frac{d\phi}{dx} + q_p - \frac{h}{2} r = 0 \quad \text{at } \Gamma_q \quad (7)$$

Register for free at <https://www.scipedia.com> to download the version without the watermark

The governing equations of the problem are completed with the standard Dirichlet condition prescribing the value of  $\phi$  at the boundary  $\Gamma_\phi$ .

The underlined terms in Equations (5) and (7) introduce the necessary stabilization in the discrete solution using whatever numerical scheme.

The time dimension can be simply accounted for the FIC method by considering the balance equation in a space–time slab domain. Application of the FIC method to the transient convection–diffusion equations and to fluid flow problems can be found in References [23, 28–33]. Quite generally the FIC equation can be written for any problem in mechanics as [22]

$$r_i - \frac{h_j}{2} \frac{\partial r_i}{\partial x_j} - \frac{\delta}{2} \frac{\partial r_i}{\partial t} = 0, \quad \begin{matrix} i = 1, n_b \\ j = 1, n_d \end{matrix} \quad (8)$$

where  $r_i$  is the  $i$ th standard differential equation of the infinitesimal theory,  $h_j$  are characteristic length parameters,  $\delta$  is a time stabilization parameter and  $t$  the time;  $n_b$  and  $n_d$  are, respectively, the number of balance equations and the number of space dimensions of the problem (i.e.,  $n_d = 2$  for 2D problems, etc.). Indeed for the transient case the initial boundary conditions must be specified. The usual sum convention for repeated indexes is used in the text unless otherwise specified.

For example, in the case of the convection–diffusion problem  $n_b = 1$  and Equation (8) is particularized as

$$r - \frac{h_j}{2} \frac{\partial r}{\partial x_j} - \frac{\delta}{2} \frac{\partial r}{\partial t} = 0, \quad j = 1, n_d \quad (9)$$

with

$$r := - \left( \frac{\partial \phi}{\partial t} + v_j \frac{\partial \phi}{\partial x_j} \right) + \frac{d}{dx_j} \left( k \frac{d\phi}{dx_j} \right) + Q$$

For a transient solid mechanics problems Equation (9) applies with  $n_b = n_d$  and

$$r_i := -\rho \frac{\partial^2 u_i}{\partial t^2} + \frac{\partial \sigma_{ij}}{\partial x_j} + b_i, \quad i, j = 1, n_d \quad (10)$$

where  $u_i$  are the displacements,  $\sigma_{ij}$  are the stresses and  $b_i$  the external body forces.

The modified Neumann boundary conditions in the FIC formulation can be written in the general case as [22]

$$q_{ij}n_j - \bar{t}_i - \frac{h_j}{2}n_jr_i = 0 \quad \text{on } \Gamma_q, \quad i = 1, n_b, \quad j = 1, n_d \quad (11)$$

where  $q_{ij}$  are the generalized ‘fluxes’ (such as the heat fluxes in a thermal problem or the stresses in solid or fluid mechanics),  $\bar{t}_i$  are the prescribed values of the boundary fluxes and  $n_j$  are the components of the outward normal to the Neumann boundary  $\Gamma_q$ .

In Equations (8) and (11) we have underlined once more the terms introduced by the FIC approach which are essential for deriving stabilized numerical formulations.

Register for free at <https://www.scipedia.com> to download the version without the watermark

### 3. GENERAL FIC EQUATIONS FOR STEADY-STATE CONVECTIVE–DIFFUSIVE PROBLEMS

Application of the FIC procedure to a general multidimensional steady-state convective–diffusive problem leads to the following governing equations [22]:

$$r - \frac{1}{2} \underline{\mathbf{h}^T \nabla r} = 0 \quad \text{in } \Omega \quad (12)$$

with the boundary conditions

$$\phi - \bar{\phi} = 0 \quad \text{on } \Gamma_\phi \quad (13a)$$

$$\mathbf{n}^T \mathbf{D} \nabla \phi + \bar{q}_n - \frac{1}{2} \underline{\mathbf{h}^T \mathbf{n} r} = 0 \quad \text{on } \Gamma_q \quad (13b)$$

where  $\Gamma_\phi$  and  $\Gamma_q$  are the Dirichlet and Neumann boundaries where the variable  $\phi$  and the outgoing normal diffusive flux are prescribed to values  $\bar{\phi}$  and  $\bar{q}_n$ , respectively. The modified equation (13b) is obtained by invoking higher-order balance of fluxes in a finite domain next to the Neumann boundary [22]. In above equations

$$r := -\mathbf{v}^T \nabla \phi + \nabla^T \mathbf{D} \nabla \phi + Q \quad (14)$$

where  $\mathbf{v}$  is the divergence-free velocity vector,  $\mathbf{D}$  is the diffusivity matrix,  $\nabla$  is the gradient operator,  $Q$  is the external source term and  $\mathbf{n}$  is the normal vector. Vector  $\mathbf{h}$  is the *characteristic length* vector. For 2D problems  $\mathbf{h} = [h_x, h_y]^T$ , where  $h_x$  and  $h_y$  are characteristic distances along the sides of the rectangular domain where higher-order balance of fluxes is enforced [22].

The underlined terms in Equations (12) and (13b) introduce the necessary stabilization in the numerical solution of the convective–diffusive problem using FD, FE, FV and meshless methods [4, 22–26]. As an example the FE formulation will be presented next.

### 3.1. Finite element discretization

A finite element interpolation of the unknown  $\phi$  can be written as

$$\phi \simeq \hat{\phi} = \sum N_i \hat{\phi}_i \quad (15)$$

where  $N_i$  are the shape functions and  $\hat{\phi}_i$  are the nodal values of the approximate function  $\hat{\phi}$  [1].

Application of the Galerkin FE method to Equations (12)–(13b) gives, after integrating by parts the term  $\nabla r$  (and neglecting the space derivatives of  $\mathbf{h}$ )

$$\int_{\Omega} N_i \hat{r} \, d\Omega - \int_{\Gamma_q} N_i (\mathbf{n}^T \mathbf{D} \nabla \hat{\phi} + \bar{q}_n) \, d\Gamma + \sum_e \frac{1}{2} \int_{\Omega^e} \mathbf{h}^T \nabla N_i \hat{r} \, d\Omega = 0 \quad (16)$$

The last integral in Equation (16) has been expressed as a sum of the element contributions to allow for interelement discontinuities in the term  $\nabla \hat{r}$ , where  $\hat{r} = r(\hat{\phi})$  is the residual of the FE approximation of the infinitesimal governing equations.

Note that the residual terms have disappeared from the Neumann boundary  $\Gamma_q$ . This is due to taking into account the FIC terms in Equation (13b).

Integrating by parts the diffusive terms in the first integral of (16) leads to

$$\int_{\Omega} N_i [\mathbf{v} \cdot \nabla \phi + \nabla \cdot (\mathbf{D} \nabla \phi)] \, d\Omega - \sum_e \frac{1}{2} \int_{\Omega^e} \mathbf{h} \cdot \nabla N_i \hat{r} \, d\Omega - \int_{\Omega} N_i Q \, d\Omega + \int_{\Gamma_q} N_i \bar{q}_n \, d\Gamma = 0 \quad (17)$$

In matrix form

$$\mathbf{K} \mathbf{a} = \mathbf{f} \quad (18)$$

Matrix  $\mathbf{K}$  and vector  $\mathbf{f}$  are assembled from the element contributions given by

$$K_{ij}^e = \int_{\Omega^e} \left[ N_i \mathbf{v}^T \nabla N_j + \nabla^T N_i \left( \mathbf{D} + \frac{1}{2} \mathbf{h} \mathbf{v}^T \right) \nabla N_j \right] \, d\Omega - \frac{1}{2} \int_{\Omega^e} \mathbf{h}^T \nabla N_i \nabla (\mathbf{D} \nabla N_j) \, d\Omega \quad (19)$$

$$f_i^e = \int_{\Omega^e} \left[ N_i + \frac{1}{2} \mathbf{h}^T \nabla N_i \right] Q \, d\Omega - \int_{\Gamma_q^e} N_i \bar{q}_n \, d\Gamma \quad (20)$$

Note that the method introduces in  $\mathbf{K}$  an additional diffusivity matrix given by  $\frac{1}{2} \mathbf{h} \mathbf{v}^T$ . Also the second integral of Equation (19) vanishes for linear approximations. The same happens with the second term of the first integral of Equation (20) when  $N_i$  is linear and  $Q$  is constant. The evaluation of these integrals is mandatory in any other case.

### 3.2. Equivalence with the SUPG method

We could further assume that the direction of vector  $\mathbf{h}$  is *parallel* to the velocity  $\mathbf{v}$ , i.e.  $\mathbf{h} = h(\mathbf{v}/|\mathbf{v}|)$  where  $h$  is a characteristic length. Under these conditions, Equation (16) reads

$$\int_{\Omega} N_i \hat{r} \, d\Omega - \int_{\Gamma_q} N_i (\mathbf{n}^T \mathbf{D} \nabla \hat{\phi} + \bar{q}_n) \, d\Omega + \sum_e \int_{\Omega^e} \frac{h}{2|\mathbf{v}|} \mathbf{v}^T \nabla N_i \hat{r} \, d\Omega = 0 \quad (21)$$

Equation (21) coincides precisely with the so-called streamline-upwind-Petrov–Galerkin (SUPG) method. The ratio  $h/2|\mathbf{v}|$  has dimensions of time and it is usually termed element *intrinsic time* parameter  $\tau$ . It can be shown that the definition of  $\mathbf{h}$  parallel to  $\mathbf{v}$  is equivalent to introducing an artificial diffusion of value  $h|\mathbf{v}|/2$  along the streamlines [1, 6, 22]. The element characteristic length  $h$  is computed in practice by an heuristic extension of the optimal value for the 1D problem. A more consistent procedure is given in the next section.

It is important to note that the SUPG expression is a *particular case* of the more general FIC formulation. This explains the limitations of the SUPG method to provide stabilized numerical results in the vicinity of sharp gradients of the solution transverse to the flow direction [1]. In general, the direction of  $\mathbf{h}$  is not coincident with that of  $\mathbf{v}$  and the components of  $\mathbf{h}$  introduce the necessary stabilization along the streamlines and the transverse directions to the flow. In this manner, the FIC method reproduces the best-features of the so-called stabilized discontinuity-capturing schemes [34, 35].

## 4. COMPUTATION OF THE CHARACTERISTIC LENGTH

The computation of the characteristic length is a crucial step as its value affect to the stability (and accuracy) of the numerical solution. This problem is common to all stabilized FE methods and different approaches to compute the stabilization parameters using typically extensions of the optimal values for simple 1D case (giving a nodally exact solution) have been proposed [1, 6, 8, 13, 16, 36].

One of the relevant aspect of the FIC formulation is that the characteristic length parameters can be accurately computed from the FIC governing equations. In general, the characteristic lengths are a function of the numerical solution values and this introduces a non-linearity in the computational process. An iterative scheme for computing the characteristic lengths based on a *diminishing residual technique* was proposed in References [22–24]. Here a simpler procedure leading to an accurate stabilized solution for multidimensional problems is proposed.

### 4.1. The 1D convection–diffusion equation

Consider the simpler steady-state 1D convection–diffusion problem. The FIC equation for the discrete problem can be written as

$$\hat{r} - \frac{h}{2} \frac{d\hat{r}}{dx} = r_{\Omega} \quad (22)$$

where  $r_{\Omega}$  is the residual of the modified governing equation and  $\hat{r}$  is given (for a zero source) by

$$\hat{r} = -v \frac{d\hat{\phi}}{dx} + k \frac{d^2 \hat{\phi}}{dx^2} \quad (23)$$

From Equation (22) it is deduced that a value of  $h$  ensuring convergence of the numerical solution ( $r_\Omega \rightarrow 0$ ) must satisfy the following condition:

$$h \left( \frac{d\hat{r}}{dx} \right) \leq 2\hat{r} \quad (24)$$

Equation (24) assumes that  $\hat{r}$  has a positive value. For  $\hat{r} < 0$  the inequality sign must be reversed in Equation (24) and hereonwards.

Substituting Equation (23) into (24) and neglecting the third derivatives of  $\phi$  gives

$$h \left( \frac{d^2\hat{\phi}}{dx^2} \right) \geq 2 \frac{d\hat{\phi}}{dx} - \frac{2k}{u} \frac{d^2\hat{\phi}}{dx^2} \quad (25)$$

The expression of  $\alpha$  given by Equation (25) is non-linear and depends on the gradient and the curvature of the numerical solution as expected. An iterative algorithm for computing  $h$  in convection–diffusion problems based on a *residual diminishing technique* was presented in References [22–24].

Equation (25) can be used to estimate the characteristic length for an individual element as follows. First we define the dimensionless stabilization parameter for the element as  $\alpha = h/l^e$ , where  $l^e$  is the element length. Introducing this expression into Equation (25) gives

$$\alpha \left( \frac{d\hat{\phi}}{dx} \right)^{(e)} \geq \frac{2}{l^e} \left( \frac{d\hat{\phi}}{dx} \right)^{(e)} - \frac{1}{\gamma} \left( \frac{d\hat{\phi}}{dx} \right)^{(e)} \quad (26)$$

where  $(\cdot)^{(e)}$  denotes values at the element level and the element Peclet number  $\gamma = ul^e/2k$ . The derivatives in Equation (26) are now approximated from the finite element solution as  $(d\hat{\phi}/dx)^{(e)} \simeq O(\hat{\phi}_i/2)$  and  $(d^2\hat{\phi}/dx^2)^{(e)} \simeq O(\hat{\phi}_i/l^e)$  where  $\hat{\phi}_i$  is a representative nodal value. Substituting this approximation into Equation (26) and dividing by the derivative of  $\hat{\phi}$  for practical computations

$$\begin{aligned} \alpha &= (1 + \varepsilon)\alpha_c \quad \text{for } |\gamma| > 1 \\ \alpha &= 0 \quad \text{for } |\gamma| \leq 1 \end{aligned} \quad (27)$$

where  $\varepsilon$  is a very small value (we usually take  $\varepsilon = 10^{-6}$ ) and

$$\alpha_c = \text{sign}(v) \left( 1 - \frac{1}{|\gamma|} \right) \quad (28)$$

which coincides with the *critical value* of the stabilization parameter ensuring a stable numerical solution [1, 2, 22, 23]. Note that above derivation emanates from the FIC differential equation prior to any discretization step.

#### 4.2. Computation of the characteristic length vector

The ideas from the simple 1D case are extended next to derive an iterative procedure for computing the characteristic length vector for 2D and 3D problems. The method allows to obtain stabilized solutions in problems with *sharp gradients* in one or two steps.



The algorithm is based in the split of vector  $\mathbf{h}$  as

$$\mathbf{h} = \mathbf{h}_s + \mathbf{h}_t \quad (29)$$

where  $\mathbf{h}_s$  and  $\mathbf{h}_t$  are characteristic length vectors in the direction of the velocity and in a transverse direction, respectively.

*Evaluation of the streamline characteristic length vector  $\mathbf{h}_s$ .* For  $\mathbf{h}_s$  the classical definition of the SUPG method is chosen, i.e.

$$\mathbf{h}_s = \frac{h_s}{|\mathbf{v}|} \mathbf{v} \quad (30)$$

The value of  $h_s$  can be computed as follows. The discretized form of Equation (12) can be written using Equations (29) and (30) and neglecting the contribution of  $\mathbf{h}_t$  as

$$\hat{r} - h_s \frac{\mathbf{v}^T}{2|\mathbf{v}|} \nabla \hat{r} = r_s \quad (31)$$

For  $r_s = 0$  this gives the *critical value* of  $h_s$  as

$$h_s = \frac{2\hat{r}|\mathbf{v}|}{\mathbf{v}^T \nabla \hat{r}} \quad (32)$$

Substituting the expression of  $\hat{r}$  from Equation (14) into (32) and neglecting third-order derivative terms gives

$$h_s = \frac{\left[ 2v_i(\partial\hat{\phi}/\partial x_i) - \sum_i 2k_i(\partial^2\hat{\phi}/\partial x_i\partial x_i) - 2Q \right] |\mathbf{v}|}{v_i v_j (\partial^2\hat{\phi}/\partial x_i\partial x_j) - v_i \partial Q/\partial x_i} \quad i, j = 1, n_d \quad (33)$$

Register for free at <https://www.scipedia.com> to download the version without the watermark

In Equation (33) we have assumed the conductivities  $k_i$  to be constant.

Equation (33) allows to compute the critical value of  $h_s$  at any point within the mesh. It can be checked that Equation (33) reduces to  $h = \text{sign}(v)(1 - 1/|\gamma|)l^e$  for the 1D case (with  $Q = 0$ ).

The presence of the derivatives of  $\hat{\phi}$  in Equation (33) introduces a non-linearity in the computation of  $h_s$ . The evaluation of the second derivatives of  $\hat{\phi}$  at the Gauss points of linear elements can be performed by nodal projection and smoothing of the first derivatives field [37, 38].

For practical purposes a simplified *linear* expression for  $h_s$  can be derived by assuming the velocity values to be large compared to those of the conductivity and the source terms (i.e. the so called *convective limit*). This gives for linear elements (assuming  $Q$  to be constant)

$$h_s \simeq l_s = \frac{2v_i(\partial\hat{\phi}/\partial x_i)|\mathbf{v}|}{v_i v_j (\partial^2\hat{\phi}/\partial x_i\partial x_j)} \simeq \frac{v_k}{l_k} |\mathbf{v}| \left[ \frac{v_i v_j}{l_i l_j} \right]^{-1}, \quad i, j, k = 1, n_d \quad (34)$$

when  $l_i$  is a typical element dimension along the  $i$ th axis (see Figure 2). Figure 3 shows some examples of the computation of  $h_s$  in linear triangular and rectangular elements. Note that for the 1D case Equation (34) gives  $h_s = l^e$ .

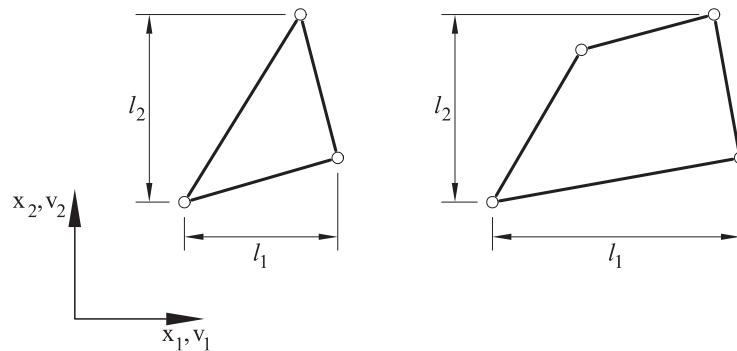
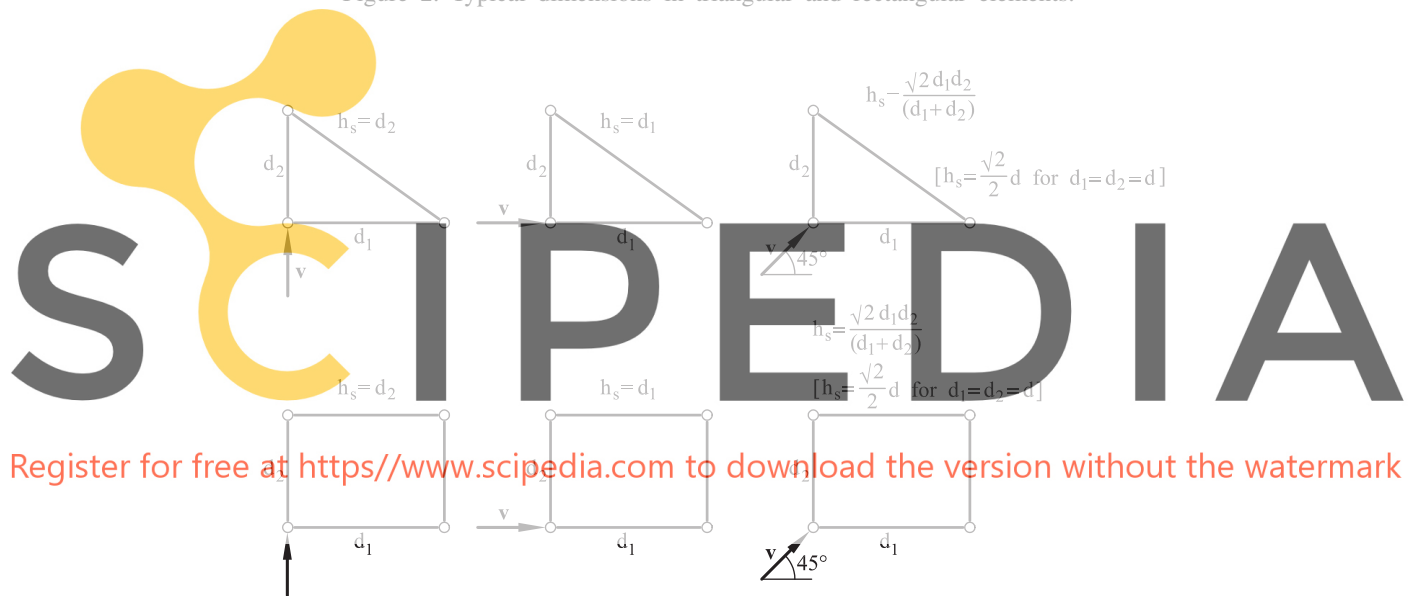


Figure 2. Typical dimensions in triangular and rectangular elements.

Figure 3. Some values of the streamline characteristic length  $h_s$  for linear triangular and rectangular elements.

A value of  $h_s$  for all the range of velocities can be computed as

$$h_s = \alpha_s l_s \quad \text{where } l_s \text{ is given by Equation (34)} \quad (35)$$

$$\alpha_s = 1 - \frac{1}{\gamma_s} \quad \text{for } \gamma_s > 1$$

$$\alpha_s = 0 \quad \text{for } \gamma_s \leq 1 \quad (36)$$

where  $\gamma_s = |\mathbf{v}|l_s/2k$  and  $k = (\sum_{i=1}^n k_i^2)^{1/2}$ .

The same procedure can be used to compute  $\mathbf{h}_s$  for higher-order elements.

*Evaluation of the transverse characteristic vector  $\mathbf{h}_t$ .* For  $\mathbf{h}_t$  we take

$$\mathbf{h}_t = \frac{h_t}{|\nabla \hat{\phi}|} \nabla \hat{\phi} \quad (37)$$

Therefore, vector  $\mathbf{h}_t$  is assumed to be parallel to the *direction of the gradient of the approximate solution  $\hat{\phi}$* . This assumption introduces a non linearity in the computation process.

The value of  $h_t$  can be estimated as follows. Substituting Equation (37) into the discretized form of Equation (12) gives

$$r_\Omega = r_s - \frac{1}{2} \mathbf{h}_t^T \nabla \hat{r} \quad (38)$$

where  $r_s$  is defined by Equation (31). Obviously for the initial solution  $\mathbf{h}_t = \mathbf{0}$  and  $r_\Omega = r_s$ .

If  $r_\Omega \neq 0$  after the first step, then we can compute  $\mathbf{h}_t$  in order to ensure that  $r_\Omega = 0$ , i.e.

$$r_s - \frac{1}{2} \mathbf{h}_t^T \nabla \hat{r} = 0 \quad (39)$$

Substituting the expression of  $\mathbf{h}_t$  of Equation (37) into (39) gives

$$h_t = \frac{2r_s |\nabla \hat{\phi}|}{\nabla^T \hat{\phi} \nabla \hat{r}} \quad (40)$$

The introduction of  $\mathbf{h}_t$  in the Galerkin equations gives the following additional term

$$\int_{\Omega^e} \left( \frac{r_s^2}{\nabla^T \hat{\phi} \nabla \hat{r}} \right) \nabla^T \hat{\phi} \nabla N_i \, d\Omega \quad (41)$$

This is equivalent to introducing an *isotropic diffusion* over each element of value

$$k_t = \frac{r_s^2}{|\nabla^T \hat{\phi} \nabla \hat{r}|} \quad (42)$$

The absolute value is taken in the denominator in order to ensure a positive value of  $k_t$ .

The expressions of  $h_s$  and  $h_t$  are the basis for an iterative scheme to obtain a stable solution which is described in a next section.

Before that, a very good approximation for  $\mathbf{h}_t$  at elements adjacent to outflow boundaries is proposed.

*Boundary simplification of  $\mathbf{h}_t$ .* Equation (37) can be approximated in elements adjacent to the boundary (where the sharper gradients usually occur) simply by accepting that  $\mathbf{h}_t$  is constant over the element and that the direction of  $\nabla \hat{\phi}$  coincides with that of the normal vector exterior to the side (or face) belonging to the boundary. Vector  $\mathbf{h}_t$  in these elements is defined as

$$\mathbf{h}_t = h_t \mathbf{n} \quad (43)$$

In elements sharing more than one side (or face) with a boundary line,  $\mathbf{h}_t$  is computed as

$$\mathbf{h}_t = \sum_{i=1}^{n_l} h_{ti} \mathbf{n}_i \quad (44)$$

where  $n_l$  is the number of sides (or faces) belonging to the boundary ( $n_l \leq 2$  in 2D).

In practice it is only necessary to introduce  $\mathbf{h}_t$  on the outflow boundaries (where  $\mathbf{v}^T \mathbf{n} > 0$ ). The characteristic length distances  $h_{t_i}$  are computed in these boundaries as

$$h_{t_i} = |d_{t_i} - \mathbf{h}_s^T \mathbf{n}_i| \alpha_{t_i} \quad (45)$$

$$d_{t_i} = \max |\mathbf{n}_i^T \mathbf{l}_j|, \quad j = 1, 2, \dots, n_s \quad (46)$$

where  $n_s$  is the number of element sides,  $l_j$  is the length of the  $j$ th element side on the boundary and

$$\alpha_{t_i} = 1 - \frac{1}{\gamma_{t_i}} \quad \text{for } \gamma_{t_i} > 1 \quad (47)$$

$$\alpha_{t_i} = 0 \quad \text{for } \gamma_{t_i} \leq 1 \quad \text{with } \gamma_{t_i} = \frac{|\mathbf{v}^T \mathbf{n}_i| d_{t_i}}{2k} \quad (48)$$

In elements with only one node on the boundary (as it occurs in non structured grids and in triangular meshes) we take  $n_l = 1$  and for  $\mathbf{n}_i$  the boundary normal at the node.

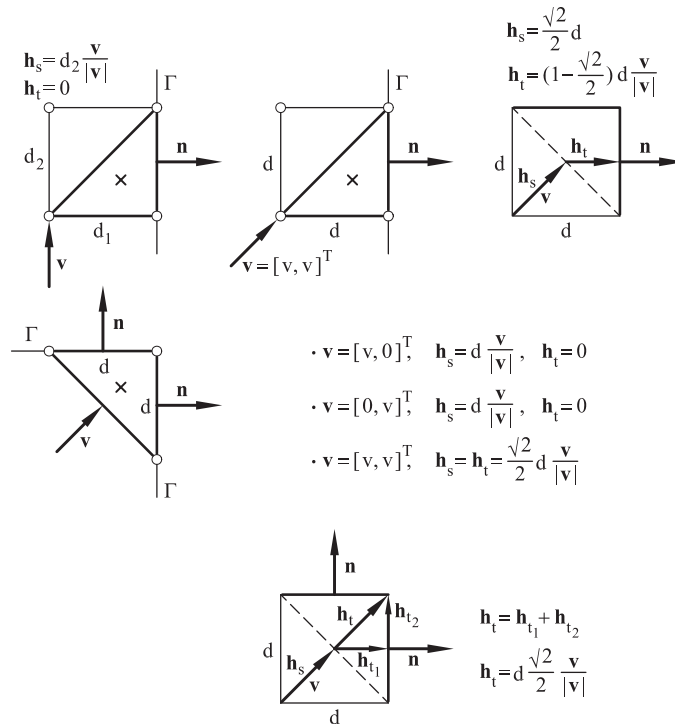


Figure 4. Some values of the streamline and transverse characteristic length vectors for linear triangles adjacent to the boundary.

Equation (45) accounts for the correction of  $h_{ti}$  due to the simultaneous application of vector  $\mathbf{h}_s$ . Figure 4 shows some examples of the computation of  $\mathbf{h}_t$  in linear triangles adjacent to the boundary.

The combination of Equations (30), (33) and (43)–(46) allows to solve convection–diffusion problems with sharp boundary layers in *one single step*. Note that the resulting problem is *linear*.

If numerical instabilities still exist due to sharp gradients in interior zones, the expression of  $\mathbf{h}_t$  of Equation (37) should be used for the elements adjacent to the unstable zones.

#### 4.3. Iterative algorithm for computing the characteristic length vector $\mathbf{h}$

The computational scheme can be summarized as follows:

1. Solve the convection–diffusion problem using the expressions of  $\mathbf{h}_s$  and  $\mathbf{h}_t$  given by Equations (30) and (43). This step provides a stabilized solution along the streamline direction and along the boundaries where high gradients can occur.
2. Check the value of  $\hat{r}_\Omega = \hat{r} - \frac{1}{2} \mathbf{h}^T \nabla \hat{r}$  in all elements (in average sense). If high values of  $\hat{r}_\Omega$  are detected in some elements, solve step 3.
3. Repeat step 1 using for the elements adjacent to the unstable zones the value of  $\mathbf{h}_t$  given by Equation (37). Go to step 2.

The process is repeated until the values of the residual  $\hat{r}_\Omega$  can be considered acceptable.

## 5. EXAMPLES

### 5.1. 2D stationary convection–diffusion problem with diagonal velocity, zero source and uniform Dirichlet conditions

The steady-state convection–diffusion equation is solved in a domain of unit size (Figure 5) with

$$k_x = k_y = 1, \quad \mathbf{v} = 10^{10} [1, 1]^T, \quad Q = 0 \quad (49)$$

The following Dirichlet conditions are assumed

$$\phi = 0 \quad \text{on the lines } x = 0 \quad \text{and} \quad y = 0$$

$$\phi = 100 \quad \text{on the lines } x = 1 \quad \text{and} \quad y = 1$$

The expected solution is a uniform distribution of  $\phi = 0$  over the domain except in the vicinity of the boundaries  $x = 1$  and  $y = 1$  where a boundary layer is formed.

The domain is discretized with a uniform mesh of 400 four node quadrilaterals (Figure 5).

The solution has been obtained in one single step using the value of  $\mathbf{h}_s$  and  $\mathbf{h}_t$  given by Equations (30) and (43), respectively. Figures 5 and 6 show that the two boundary layers expected are perfectly captured without any oscillation.

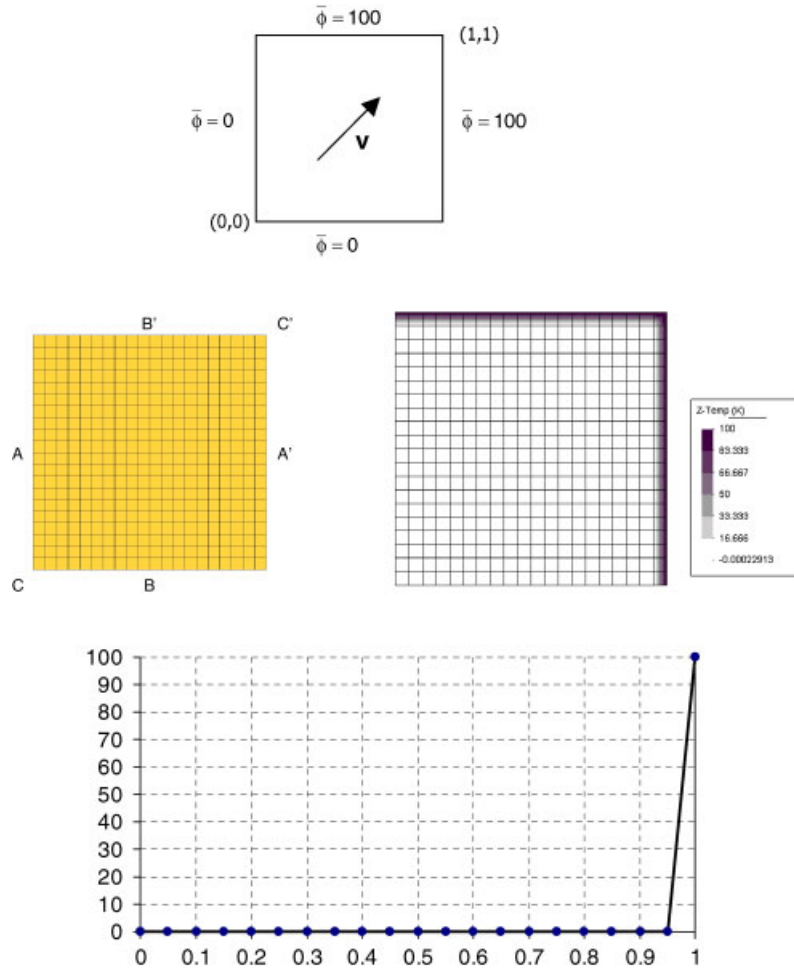


Figure 5. Convection–diffusion problem with uniform Dirichlet conditions. One step solution. Distribution of  $\phi$  along the lines  $AA'$  and  $BB'$ .

Note that a solution of the same quality using standard discontinuity capturing methods would have required at least two iterations.

### 5.2. 2D stationary convection–diffusion problem with diagonal velocity, zero source and non-uniform Dirichlet conditions

The convection–diffusion equation is solved again in a square domain of unit size with

$$\mathbf{v} = 10^6[5, -9]^T, \quad k_x = k_y = 1, \quad Q = 0, \quad \bar{\phi}(x, y) = \begin{cases} 100 & \text{if } (x, y) \in \Gamma_{\phi_1} \\ 0 & \text{if } (x, y) \in \Gamma_{\phi_2} \end{cases}$$

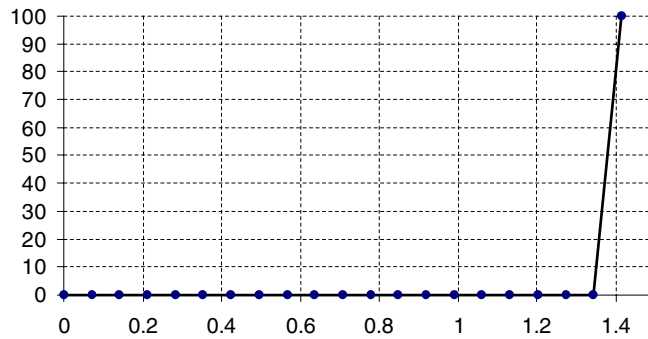


Figure 6. Convection–diffusion problem with uniform Dirichlet conditions. One step solution. Distribution of  $\phi$  along the diagonal line  $CC'$ .

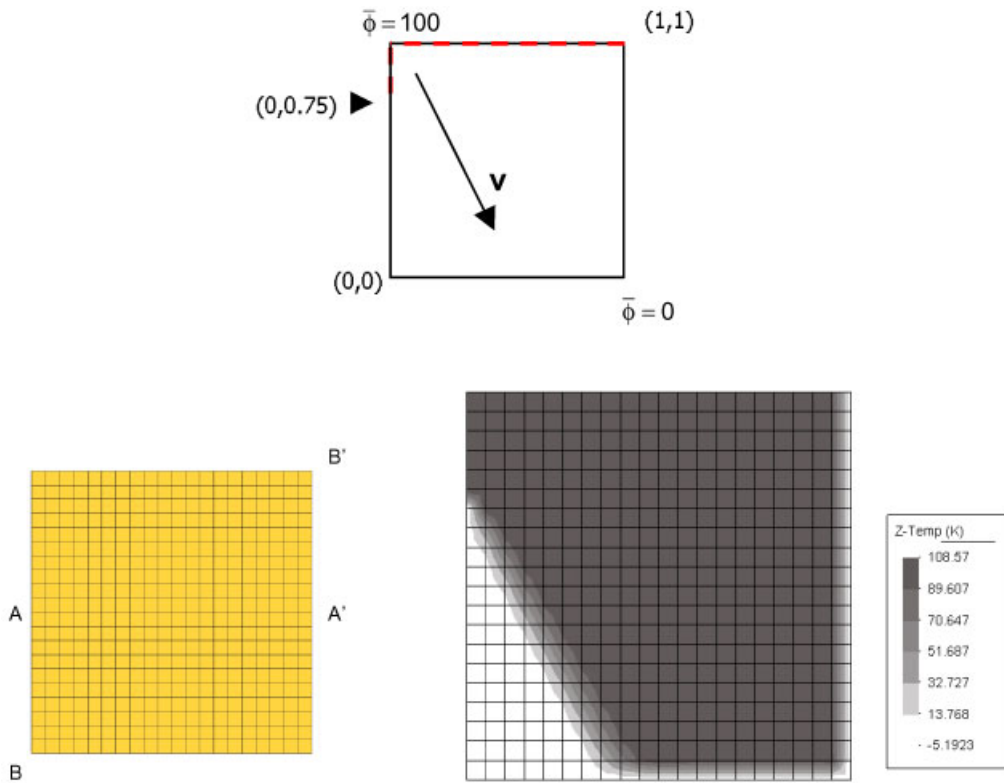


Figure 7. Convection–diffusion problem with non-uniform Dirichlet conditions. Distribution of  $\phi$  after the first step.

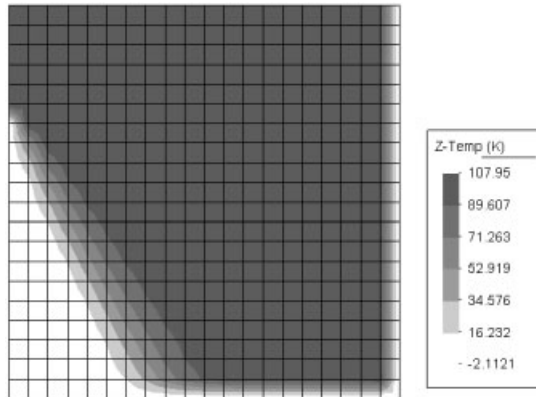


Figure 8. Convection–diffusion problem with non-uniform Dirichlet conditions. Distribution of  $\phi$  after the first iteration.

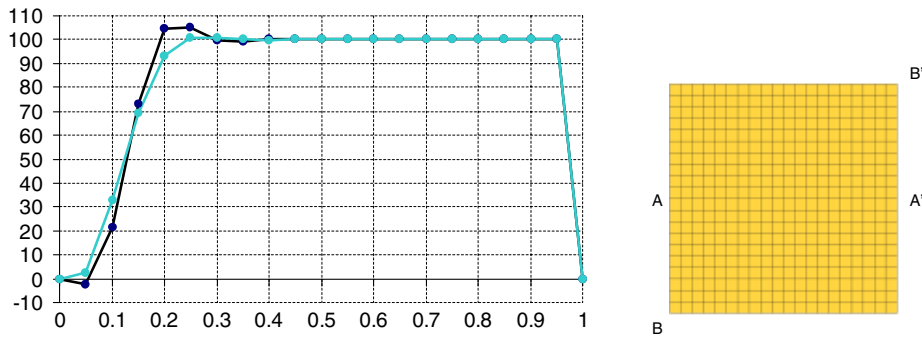


Figure 9. Convection–diffusion problem with non-uniform Dirichlet conditions. Distribution of  $\phi$  along the horizontal mid-line  $AA'$  obtained in the first step (oscillatory solution—black line) and after the first iteration (solution without oscillations—greyline).

with the following non-uniform Dirichlet conditions

$$\Gamma_{\phi_1} = \{(x, y)/x \in [0, 1], y = 1\} \cup \left\{ (x, y)/x = 0, y \in \left[ \frac{3}{4}, 1 \right] \right\}$$

$$\Gamma_{\phi_2} = \partial\Omega/\Gamma_{\phi_1}$$

The mesh of 400 four node quadrilaterals shown in Figure 7 has been used.

The problem has been solved with the iterative algorithm described in the previous section. Figure 7 shows the distribution of  $\phi$  obtained in the first step with the values of  $\mathbf{h}_s$  and  $\mathbf{h}_t$  of Equations (30) and (43), respectively. Note that the sharp layers adjacent to the boundary are perfectly captured. It however remains a zone in the interior of the domain where an oscillatory solution is obtained due to the sharp gradients of  $\phi$  and this leads to high values of the residual in this region.



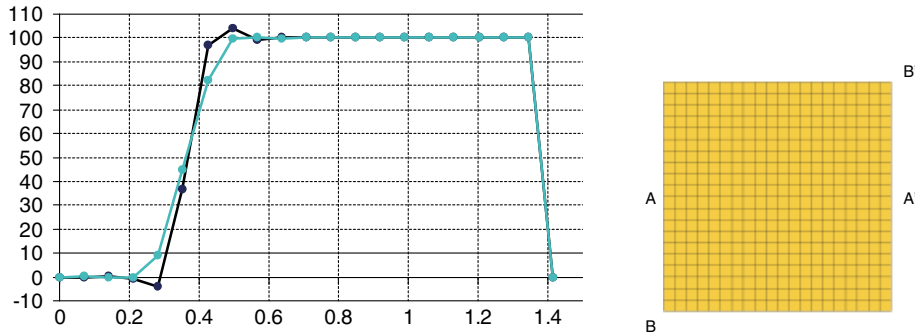


Figure 10. Convection–diffusion problem with non-uniform Dirichlet conditions. Distribution of  $\phi$  along the diagonal line  $BB'$  after the first step (oscillatory solution—black line) and after the first iteration (solution without oscillations—greyline).

A second solution is next obtained using the value of  $\mathbf{h}_t$  of Equation (37) in the element adjacent to the unstable region. This yields a stabilized solution in the whole domain (Figure 8). Figures 9 and 10, respectively show the distributions of  $\phi$  along the horizontal line  $AA'$  and the diagonal line  $BB'$  obtained in the first step and after the first iteration. Note that the algorithm eliminates the oscillations induced by the sharp gradients in the interior of the domain.

Figures 11 and 12 show a similar solution for the same example using a non-structured mesh of four node quadrilaterals. Note that the algorithm captures the boundary layers in a first step and provides a stabilized distribution of  $\phi$  over the whole domain after performing an additional iteration.

## 6. AN INTERPRETATION OF THE FINITE CALCULUS METHOD

Let us consider the solution of a physical problem, such as obtaining the steady-state distribution of the temperature  $\phi$  in a domain  $\Omega$ , governed by a differential equation  $r(\phi) = 0$  in  $\Omega$  with the corresponding boundary conditions. The ‘exact’ (analytical) solution of the problem will be a function giving the sought distribution of the temperature  $\phi$  for any value of the geometrical and physical parameters of the problem. Obviously, since the analytical solution is difficult to find (practically impossible for real situations), an approximate numerical solution is found  $\phi \simeq \hat{\phi}$  by solving the problem  $\hat{r} = 0$ , with  $\hat{r} = r(\hat{\phi})$ , using a particular discretization method (such as the FEM). The temperature distribution in  $\Omega$  is now obtained for specific values of the geometrical and physical parameters. The accuracy of the numerical solution depends on the discretization parameters, such as the number of elements and the approximating functions chosen in the FEM. Figure 13 shows a schematic representation of the distributions of  $\hat{\phi}$  along a line for different discretizations  $M_1, M_2, \dots, M_n$  where  $M_1$  and  $M_n$  are the coarser and finer meshes, respectively. Obviously for  $n$  sufficiently large a good approximation of  $\phi$  will be obtained and for  $M_\infty$  the numerical solution  $\hat{\phi}$  will coincide with the ‘exact’ (and probably unreachable) analytical solution  $\phi$  at all points. Indeed in some problems the  $M_\infty$  solution can be found by a ‘clever’ choice of the discretization parameters.

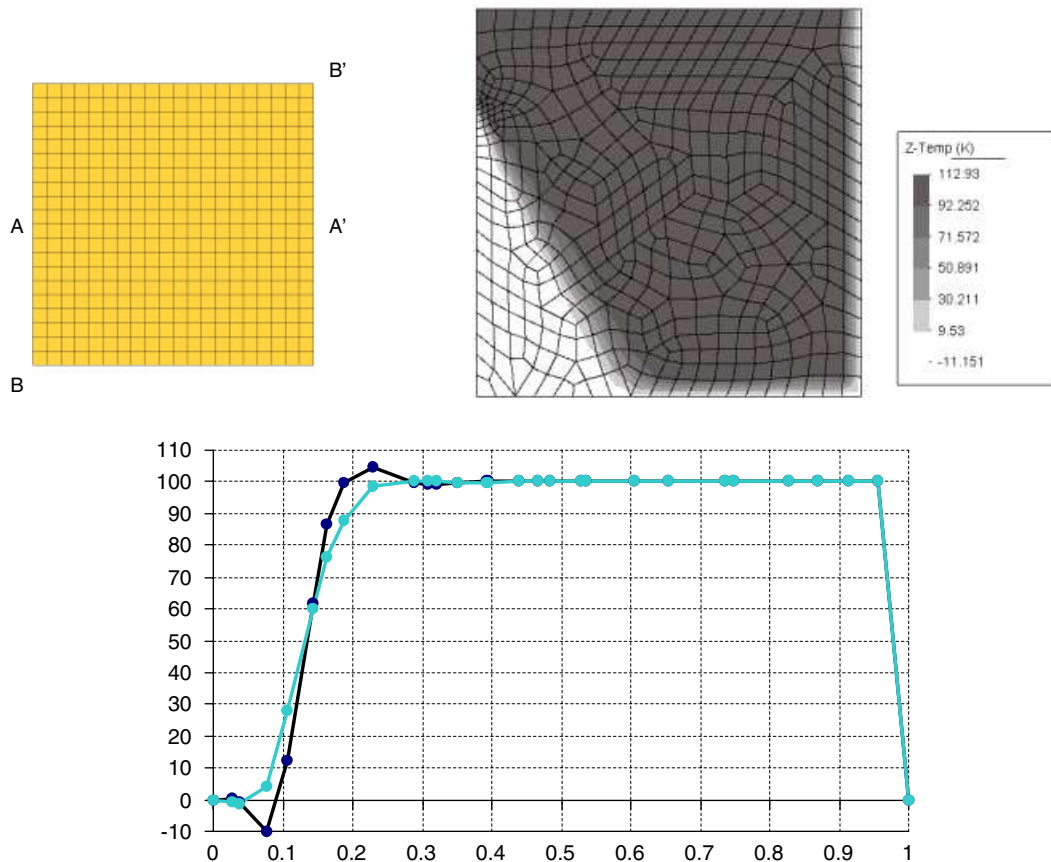


Figure 11. Convection–diffusion problem with non-uniform Dirichlet conditions. Unstructured mesh of four node quadrilaterals. Final distribution of  $\phi$  over the domain. Values of  $\phi$  along the horizontal line  $AA'$  obtained after the first step (oscillatory solution—black line) and after the first iteration (solution without oscillations—greyline).

The problem arises when for some (typically coarse) discretizations, the numerical solution provides non physical or very unaccurate values of  $\hat{\phi}$ . The numerical method is then said to be unstable. A situation of this kind is represented by curves  $M_1$  and  $M_2$  of the left-hand side of Figure 13. These unstabilities would disappear by an appropriate mesh refinement (curves  $M_3, M_4, \dots$ ) at the obvious increase of the computational cost.

In the FIC formulation the starting point are the modified differential equations of the problem, expressed by  $r - (h/2) dr/dx = 0$  in  $\Omega$  and the corresponding modified boundary conditions as previously described. The modified equations are not longer useful to find an analytical solution,  $\phi(x)$ , for the physical problem. However, the numerical solution of the FIC equation can be readily found. Moreover, by adequately choosing the values of the characteristic length parameter  $h$ , the numerical solution of the FIC equations will be always stable (physically sound) for any discretization level chosen.

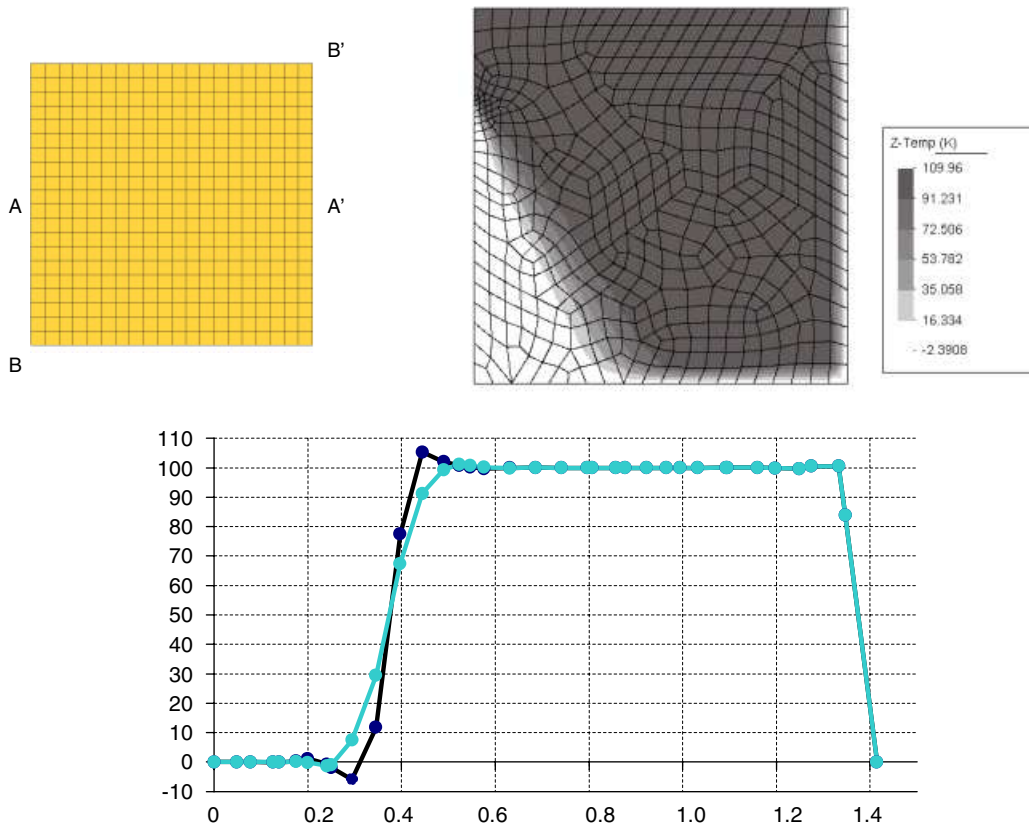


Figure 12. Convection–diffusion problem with non-uniform Dirichlet conditions. Unstructured mesh of four node quadrilaterals. Final distribution of  $\phi$  over the domain. Values of  $\phi$  along the diagonal line  $BB'$  obtained after the first (black line) and second (grey line) steps. The oscillatory solution corresponds to the first step (black line).

This process is schematically represented in Figure 13 where it is shown that the numerical oscillations for the coarser discretizations  $M_1$  and  $M_2$  disappear when using the FIC procedure.

We can therefore conclude the FIC approach allows us to obtain a *better numerical solution for a given discretization*. Indeed, as in the standard infinitesimal case, the choice of  $M_\infty$  will yield the (unreachable) exact analytical solution and this ensures the consistency of the method.

## 7. THE FIC METHOD IN INCOMPRESSIBLE FLUID MECHANICS

The FIC method can be applied to derive the modified equations of momentum, mass and energy conservation in fluid mechanics. The general form of these equations for a compressible fluid was presented in Reference [22]. We will consider here the particular case of a *viscous incompressible fluid*. The FIC equations for the momentum and mass balance in this case can be written as (neglecting time stabilization terms) [22, 29, 32]

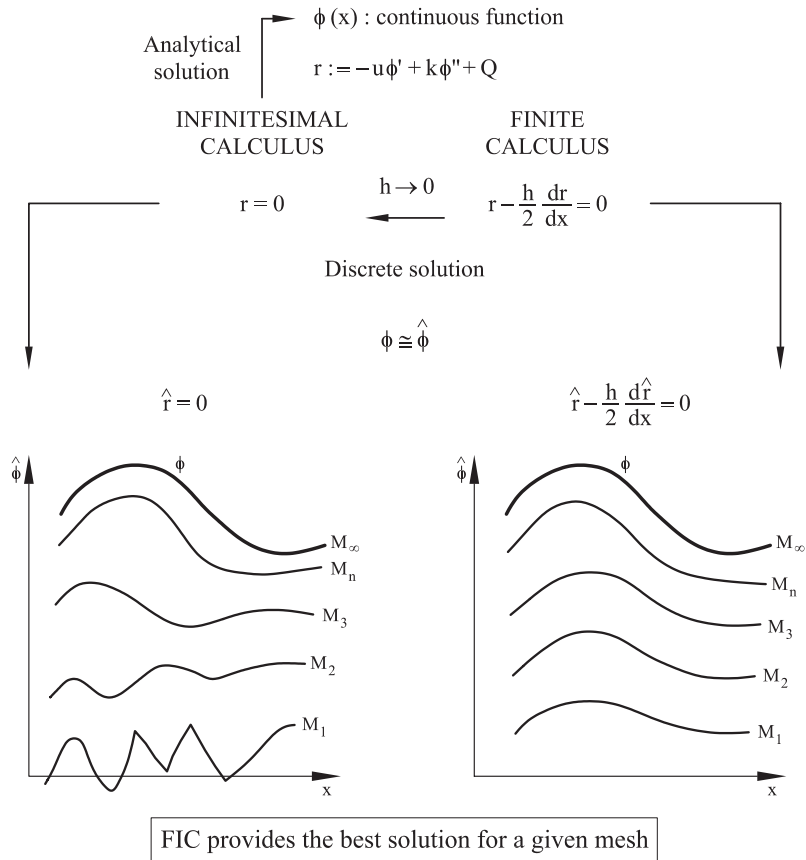


Figure 13. Schematic representation of the numerical solution of a physical problem using standard infinitesimal calculus and the finite calculus method.

*Momentum:*

$$r_{m_i} - \frac{1}{2} h_j \frac{\partial r_{m_i}}{\partial x_j} = 0 \quad (50)$$

*Mass balance:*

$$r_d - \frac{1}{2} h_j \frac{\partial r_d}{\partial x_j} = 0 \quad (51)$$

where

$$r_{m_i} = \rho \left( \frac{\partial v_i}{\partial t} + \frac{\partial(v_i v_j)}{\partial x_j} \right) + \frac{\partial p}{\partial x_i} - \frac{\partial s_{ij}}{\partial x_j} - b_i \quad (52)$$

$$r_d = \frac{\partial v_i}{\partial x_i}, \quad i, j = 1, n_d \quad (53)$$

Above  $v_i$  is the velocity along the  $i$ th global axis,  $\rho$  is the (constant) density of the fluid,  $p$  is the absolute pressure (defined positive in compression),  $b_i$  are body forces and  $s_{ij}$  are the viscous deviatoric stresses related to the viscosity  $\mu$  by the standard expression

$$s_{ij} = 2\mu \left( \dot{\epsilon}_{ij} - \delta_{ij} \frac{1}{3} \frac{\partial v_k}{\partial x_k} \right) \quad (54)$$

where  $\delta_{ij}$  is the Kronecker delta and the strain rates  $\dot{\epsilon}_{ij}$  are

$$\dot{\epsilon}_{ij} = \frac{1}{2} \left( \frac{\partial v_i}{\partial x_j} + \frac{\partial v_j}{\partial x_i} \right) \quad (55)$$

The FIC boundary conditions are written as

$$n_j \sigma_{ij} - t_i + \frac{1}{2} h_j n_j r_{m_i} = 0 \quad \text{on } \Gamma_t \quad (56)$$

$$v_j - \bar{v}_j = 0 \quad \text{on } \Gamma_u \quad (57)$$

and the initial condition  $v_j = v_j^0$  for  $t = t_0$ .

In Equation (56)  $\sigma_{ij} = s_{ij} - p\delta_{ij}$  are the total stresses,  $t_i$  and  $\bar{u}_j$  are prescribed tractions and displacements on the boundaries  $\Gamma_t$  and  $\Gamma_u$ , respectively and  $n_j$  are the components of the unit normal vector to the boundary. The sign in front of the stabilization term in Equation (56) is positive due to the definition of  $r_{m_i}$  in Equation (52).

The  $h'_i$ s in above equations are characteristic lengths of the domain where balance of momentum and mass is enforced. In Equation (56) these lengths define the domain where equilibrium of boundary tractions is established [22].

Equations (50)–(57) are the starting point for deriving stabilized finite element methods for solving the incompressible Navier–Stokes equations using an equal order interpolation for the velocity and the pressure variables.

The ‘conservative’ form of the convective terms in Equation (52) and the presence of the volumetric strain rate in the constitutive equation (54) do not take advantage of the incompressibility condition. These forms are useful at this stage for obtaining the relationship between the space derivatives of the volumetric strain rate and the momentum equations. However, the standard form of the incompressible flow equations is used for the derivation of the FEM equations.

### 7.1. Stabilized integral forms

Making use of Equations (50) and (54) it can be obtained [29, 32]

$$h_j \frac{\partial r_d}{\partial x_i} \simeq \sum_{i=1}^{n_d} \tau_i \frac{\partial r_{m_i}}{\partial x_i} \quad (58)$$

where

$$\tau_i = \left( \frac{8\mu}{3h_i^2} + \frac{2\rho u_i}{h_i} \right)^{-1} \quad (59)$$

Substituting Equation (58) into Equation (51) leads to the following expression for the stabilized mass balance equation

$$r_d - \sum_{i=1}^{n_d} \tau_i \frac{\partial r_{m_i}}{\partial x_i} = 0 \quad (60)$$

The  $\tau_i$ 's in Equation (58) are termed *intrinsic time parameters per unit mass*. Note that they take here the usual values of  $\tau_i = \alpha(h_i^2/\mu)$  ( $\alpha \simeq 2 - 3$ ) and  $\tau_i = h_i/2\rho u_i$  for the viscous limit (Stokes flow) and the inviscid limit (Euler flow), respectively. The values of  $\tau_i$  are deduced in other works from *ad hoc* extensions of the 1D advective–diffusive problem and typically  $\tau_i = \tau$  is assumed. Here they have been obtained from the general FIC formulation and this shows the possibilities of the method.

The computation of the characteristic length distances  $h_i$  can follow a similar procedure as explained for the advective–diffusive problem. For details see References [29–33].

The weighted residual form of the momentum and mass balance equations (Equations (50) and (60)) is written as

*Momentum:*

$$\int_{\Omega} \delta v_i \left[ r_{m_i} - \frac{h_j}{2} \frac{\partial r_{m_i}}{\partial x_j} \right] d\Omega + \int_{\Gamma_t} \delta v_i \left( \sigma_{ij} n_j - t_i + \frac{h_j}{2} n_j r_{m_i} \right) d\Gamma = 0 \quad (61)$$

*Mass balance:*

$$\int_{\Omega} q \left[ r_d - \sum_{i=1}^{n_d} \tau_i \frac{\partial r_{m_i}}{\partial x_i} \right] d\Omega = 0 \quad (62)$$

where  $\delta u_i$  and  $q$  are arbitrary weighting functions representing virtual velocity and virtual pressure fields.

Integrations by parts of Equations (61) and (62) leads to [29, 32].

*Momentum:*

$$\begin{aligned} & \int_{\Omega} \left[ \delta v_i \rho \left( \frac{\partial v_i}{\partial t} + v_j \frac{\partial v_i}{\partial x_j} \right) + \delta \dot{e}_{ij} (\tau_{ij} - \delta_{ij} p) \right] d\Omega - \int_{\Omega} \delta v_i b_i d\Omega - \int_{\Gamma_t} \delta v_i t_i d\Gamma \\ & + \sum_e \int_{\Omega^e} \frac{h_j}{2} \frac{\partial \delta v_i}{\partial x_j} r_{m_i} d\Omega = 0 \end{aligned} \quad (63)$$

*Mass balance:*

$$\int_{\Omega} q r_d d\Omega + \int_{\Omega} \left[ \sum_{i=1}^{n_d} \tau_i \frac{\partial q}{\partial x_i} r_{m_i} \right] d\Omega = 0 \quad (64)$$

The last integral in Equation (63) is computed as a sum of the element contributions to allow for a discontinuities in the derivative of  $r_{m_i}$  along the element interfaces.

In Equation (63)  $\delta \dot{e}_{ij} = \frac{1}{2}((\partial \delta v_i / \partial x_j) + (\partial \delta v_j / \partial x_i))$ . We also note that the standard form of the convective operator for incompressible flows is now used.

The discretization of the velocity and pressure fields using the FEM leads to the following system of equations:

$$\mathbf{M}\dot{\bar{\mathbf{v}}} + [\mathbf{K}(\mu) + \bar{\mathbf{K}}(\bar{\mathbf{v}})]\bar{\mathbf{v}} - \mathbf{G}\bar{\mathbf{p}} = \mathbf{f} \quad (65a)$$

$$\mathbf{G}^T \bar{\mathbf{v}} + \mathbf{L}(\tau_i)\bar{\mathbf{p}} = 0 \quad (65b)$$

where as usual  $(\bar{\cdot})$  denote approximate nodal vectors. In (65b)  $\mathbf{L}(\tau_i)$  is a laplacian type matrix depending on the intrinsic time parameters  $\tau_i$ . The form of the different matrices and vectors can be found in References [29, 32].

It is interesting to analyse the steady-state form of Equations (65) for the *Stokes flow* case where the convective terms are neglected ( $\bar{\mathbf{K}} = \mathbf{0}$ ). The resulting symmetric system can be written as

$$\begin{bmatrix} \mathbf{K}(\mu) & -\mathbf{G} \\ -\mathbf{G}^T & -\mathbf{L}(\tau_i) \end{bmatrix} \begin{Bmatrix} \bar{\mathbf{u}} \\ \bar{\mathbf{p}} \end{Bmatrix} = \begin{Bmatrix} \bar{\mathbf{f}} \\ \mathbf{0} \end{Bmatrix} \quad (66)$$

The stability of the numerical solution is ensured by the presence of matrix  $\mathbf{L}$  guaranteeing a positive definitiveness of the equation system *for any choice of the approximations for  $\mathbf{v}$  and  $p$* , thus overcoming the Babuska–Brezzi conditions [1]. Note that now  $\tau_i = 3h_i^2/8\mu$ .

Application of the FIC method to the FE solution of the incompressible Navier–Stokes equations accounting for free surface waves using *linear triangles and tetrahedra* can be found in References [30–33]. Meshless finite point analysis of incompressible flows using the FIC technique are reported in References [4, 5]. Extensions of the FIC method to the compressible flow equations can be found in Reference [22].

Similar governing equations to that found using the FIC method have been obtained by Ilinka *et al.* [39] for incompressible advective–diffusive and fluid flow problems by expanding in Taylor series the residuals of the original FE equations. Analogous modified equations for compressible gas flow problems have been obtained in Reference [40] using discrete Boltzman schemes. The governing equations provided by the FIC method, based on simple physical concepts of balance of fluxes and forces over a finite size domain, reproduce the particular forms of the equations obtained by these authors.

## 8. THE FIC METHOD IN QUASI-INCOMPRESSIBLE AND FULL INCOMPRESSIBLE SOLID MECHANICS

Application of the FIC method to the equations of equilibrium of forces in solid mechanics leads to the following modified governing equations (for the static case)

$$r_i - \frac{h_j}{2} \frac{\partial r_i}{\partial x_j} = 0, \quad i, j = 1, n_d \quad (67)$$

with

$$r_i := \frac{\partial \sigma_{ij}}{\partial x_j} + b_i \quad (68)$$

The deviatoric stress–strain and the strain–displacement relationships have identical form to Equations (54) and (55), respectively, substituting the viscosity  $\mu$  by the shear modulus  $G$  and the velocities  $v_i$  by the displacements  $u_i$ .

The FIC method can also be applied to derive a modified equation relating the pressure and the volumetric strain change over a finite size domain as [41]

$$\left( \frac{1}{K} p - \varepsilon_v \right) - \frac{h_k}{2} \frac{\partial}{\partial x_k} \left( \frac{1}{K} p - \varepsilon_v \right) = 0, \quad k = 1, n_d \quad (69)$$

where  $K$  is the volumetric elastic modulus and  $\varepsilon_v = \partial u_i / \partial x_i$ . Note that for an incompressible material  $K \rightarrow \infty$  and in this case Equation (69) recovers a form analogous to that of the stabilized mass balance equation in fluid mechanics (see Equation (51)).

The underlined terms in Equations (67) and (69) result from the FIC assumptions and, as usual,  $h_j$  are the characteristic length parameters. The governing equations are completed with the adequate boundary conditions. Note that, for consistency, the Neumann boundary conditions must incorporate an additional stabilization term identical to that of Equation (13b) [22, 41, 42].

Equations (67) and (69) with the adequate boundary conditions are the basis for deriving stabilized FE formulations for quasi-incompressible and full incompressible solids allowing for *equal order interpolations* of the displacement and the pressure variables.

The derivation of the FE formulation follows the same steps than in the fluid flow case. The resulting system of equation for the full incompressible case ( $K = \infty$ ) has a form identical to that of the Stokes flow problem (Equation (66)).

This formulation has been successfully applied to the static and dynamic solution of quasi-incompressible and full incompressible solid mechanics problems using three node triangles and four node quadrilaterals with equal order interpolation for the displacements and the pressure [28, 41, 42].

## 9. POSSIBILITIES OF FINITE CALCULUS FOR STRAIN LOCALIZATION

The FIC method introduces naturally higher-order derivative terms of the displacements in the equilibrium equations. These terms resemble those introduced by the Cosserat model [43] and the so-called ‘non-local’ constitutive models [43–47]. These models are typically used in order to preserve the ellipticity of the solid mechanics equations in the presence of localized high displacement gradient zones, such as shear bands and fracture lines.

For instance, the FIC governing equations for a simple 1D bar can be written (in absence of external body forces) as

$$\frac{\partial N}{\partial x} - \frac{h}{2} \frac{\partial^2 N}{\partial x^2} = 0 \quad (70)$$

where  $N$  is the axial force.

The relationship between the axial force and the elongation  $\varepsilon = du/dx$  in the softening branch can be written in incremental form as

$$\delta N = -|E_T| \delta \varepsilon = -|E_T| \frac{d(\delta u)}{dx} \quad (71)$$

where  $E_T$  is the tangent modulus of the material and  $\delta u$  is the displacement increment.



Substituting Equation (71) into (70) gives

$$\frac{d^2(\delta u)}{dx^2} - \frac{h}{2} \frac{d^3(\delta u)}{dx^3} = 0 \quad (72)$$

Equation (72) resembles the governing equations derived by Lasry and Belytschko [44] using localization limiters in the stress–strain relationship and by Schreier and Chen [45] using gradient-dependent plasticity constitutive models.

Many similarities can be found between the governing equations derived by the FIC method and those resulting from the non-local constitutive models [48]. Although in some situations the resulting governing differential equations are the same, the basic difference between the two approaches is that non-local constitutive models aim to enhance the constitutive equation by adding new terms (typically strain gradient terms), whereas the FIC method defines a new equilibrium equation applicable to all the discrete scales while preserving the features of the constitutive equation. This opens a world of possibilities for the FIC equations in solid mechanics to solve strain localization problems using standard constitutive models.

## 10. CONCLUDING REMARKS

The acceptance that the domain where the equations of balance of fluxes, forces, momentum, mass, etc. are established in mechanics has a *finite size* leads to new governing differential equations that incorporate the space and time dimensions of the balance domain. The new equations can be taken as the starting point for deriving stabilized numerical schemes based on FE, FD, FV and meshless methods for solving problems of convective transport, fluid dynamics and incompressible solids, among many others.

In the first part of the paper we have shown the possibilities of the FIC method for solving the convection–diffusion equation in cases where sharp gradients transverse to the velocity direction exist. The method proposed for computing the characteristic length vector can be easily extended for solving other problems in mechanics where sharp gradients of the solution exist such as boundary layers, shocks in compressible flows, strain localization layers in solids, etc.

In the second part of the paper we have briefly described the application of the FIC methodology for solving incompressible problems in fluid flow and solid mechanics using equal order finite element interpolations. Finally, we have outlined the possibilities of the FIC method for strain localization problems.

## ACKNOWLEDGEMENTS

The author is grateful to Profs. R. L. Taylor, O. C. Zienkiewicz, J. Miquel, M. Manzán and B. Borooman for many useful discussions. Thanks are also given to Mr. J. A. Arraez and S. Badia for the computation of the convection–diffusion examples.

## REFERENCES

1. Zienkiewicz OC, Taylor RL. *The Finite Element Method* (5th edn), vol. 1–3. Butterworth-Heinemann: Stoneham, MA, 2000.

2. Hirsch C. *Numerical Computation of Internal and External Flow*, vol. 1. Wiley: New York, 1988 (vol. 2, 1990).
3. Oñate E, Idelsohn SR, Zienkiewicz OC, Taylor RL. A finite point method in computational mechanics. Applications to convective transport and fluid flow. *International Journal for Numerical Methods in Engineering* 1996; **39**:3839–3866.
4. Oñate E, Idelsohn S. A mesh free finite point method for advective–diffusive transport and fluid flow problems. *Computational Mechanics* 1988; **21**:283–292.
5. Oñate E, Sacco C, Idelsohn S. A finite point method for incompressible flow problems. *Computing and Visualization in Science* 2000; **2**:67–75.
6. Brooks A, Hughes TJR. Streamline upwind/Petrov–Galerkin formulation for convection dominated flows with particular emphasis on the incompressible Navier–Stokes equations. *Computer Methods in Applied Mechanics and Engineering* 1982; **32**:199–259.
7. Codina R. Comparison of some finite element methods for solving the diffusion–convection–reaction equation. *Computer Methods in Applied Mechanics and Engineering* 1998; **156**:185–210.
8. Hughes TJR, Mallet M. A new finite element formulations for computational fluid dynamics: III. The generalized streamline operator for multidimensional advective–diffusive systems. *Computer Methods in Applied Mechanics and Engineering* 1986; **58**:305–328.
9. Hansbo P, Szepessy A. A velocity–pressure streamline diffusion finite element method for the incompressible Navier–Stokes equations. *Computer Methods in Applied Mechanics and Engineering* 1990; **84**:175–192.
10. Cruchaga MA, Oñate E. A generalized streamline finite element approach for the analysis of incompressible flow problems including moving surfaces. *Computer Methods in Applied Mechanics and Engineering* 1999; **173**:241–255.
11. Hughes TJR, Franca LP, Hulbert GM. A new finite element formulation for computational fluid dynamics: VIII. The Galerkin/least-squares method for advective–diffusive equations. *Computer Methods in Applied Mechanics and Engineering* 1989; **73**:173–189.
12. Tezduyar TE, Mittal S, Ray SE, Shih R. Incompressible flow computations with stabilized bilinear and linear equal order interpolation velocity–pressure elements. *Computer Methods in Applied Mechanics and Engineering* 1992; **95**:221–242.
13. Douglas J, Russell TF. Numerical methods for convection dominated diffusion problems based on combining the method of characteristics with finite element or finite difference procedures. *SIAM Journal on Numerical Analysis* 1982; **19**:871.
14. Pironneau O. On the transport-diffusion algorithm and its applications to the Navier–Stokes equations. *Numerische Mathematik* 1982; **38**:309.
15. Löhner R, Morgan K, Zienkiewicz OC. The solution of non-linear hyperbolic equation systems by the finite element method. *International Journal for Numerical Methods in Fluids* 1984; **4**:1043.
16. Zienkiewicz OC, Codina R. A general algorithm for compressible and incompressible flow. Part I: the split characteristic based scheme. *International Journal for Numerical Methods in Fluids* 1995; **20**:869–85.
17. Codina R, Vazquez M, Zienkiewicz OC. A general algorithm for compressible and incompressible flow—Part III. The semi-implicit form. *International Journal for Numerical Methods in Fluids* 1998; **27**:13–32.
18. Hughes TJR. Multiscale phenomena: Green functions, subgrid scale models, bubbles and the origins of stabilized methods. *Computer Methods in Applied Mechanics and Engineering* 1995; **127**:387–401.
19. Brezzi F, Franca LP, Hughes TJR, Russo A.  $b = \int g$ . *Computer Methods in Applied Mechanics and Engineering* 1997; **145**:329–339.
20. Codina R. Stabilization of incompressibility and convection through orthogonal sub-scales in finite element method. *Computer Methods in Applied Mechanics and Engineering* 2000; **190**:1579–1599.
21. Hauke G. A simple subgrid scale stabilized method for the advection–diffusion–reaction equation. *Computer Methods in Applied Mechanics and Engineering* 2002; **191**:2925–2948.
22. Oñate E. Derivation of stabilized equations for advective–diffusive transport and fluid flow problems. *Computer Methods in Applied Mechanics and Engineering* 1998; **151**(1–2):233–267.
23. Oñate E, Manzan M. Stabilization techniques for finite element analysis of convection diffusion problems. In *Computer Analysis of Heat Transfer*, Comini G, Sunden B (eds). WIT Press: 2000.
24. Oñate E, García J, Idelsohn SR. Computation of the stabilization parameter for the finite element solution of advective–diffusive problems. *International Journal for Numerical Methods in Fluids* 1997; **25**:1385–1407.
25. Oñate E, García J, Idelsohn SR. An alpha-adaptive approach for stabilized finite element solution of advective–diffusive problems with sharp gradients. In *New Advances in Adaptive Computer Methods in Mechanics*, Ladeveze P, Oden JT (eds). Elsevier: Amsterdam, 1998.

26. Felippa CA. Modified equations methods. *Private communication*, CIMNE, Barcelona, June 2001.
27. Oñate E, Taylor RL, Zienkiewicz OC, Rojek J. A residual correction method based on finite calculus. *Engineering Computations* 2003; **20**(5–6):629–658.
28. Oñate E, Manzan M. A general procedure for deriving stabilized space–time finite element methods for advective–diffusive problems. *International Journal for Numerical Methods in Fluids* 1999; **31**:203–221.
29. Oñate E. A stabilized finite element method for incompressible viscous flows using a finite increment calculus formulation. *Computer Methods in Applied Mechanics and Engineering* 2000; **182**(1–2):355–370.
30. Oñate E, García J. A finite element method for fluid–structure interaction with surface waves using a finite calculus formulation. *Computer Methods in Applied Mechanics and Engineering* 2001; **191**(6–7):635–660.
31. García J, Oñate E. An unstructured finite element solver for ship hydrodynamics. *Journal of Applied Mechanics* 2003; **70**:18–26.
32. Oñate E, García J, Bugada G, Idelsohn SR. A general stabilized formulation for incompressible fluid flow using finite calculus and the FEM. In *Towards a New Fluid Dynamics with its Challenges in Aeronautics*, Periaux J, Champion D, Pironneau O, Thomas Ph (eds). CIMNE: Barcelona, 2002.
33. Oñate E, García J, Idelsohn SR. Ship Hydrodynamics. In *Encyclopedia of Computational Mechanics*, Hughes T, de Borst R, Stein E (eds). Wiley: New York, 2004, to be published.
34. Hughes TJR, Mallet M. A new finite element formulations for computational fluid dynamics: IV. A discontinuity capturing operator for multidimensional advective–diffusive system. *Computer Methods in Applied Mechanics and Engineering* 1986; **58**:329–336.
35. Codina R. A discontinuity-capturing crosswind dissipation for the finite element solution of the convection–diffusion equation. *Computer Methods in Applied Mechanics and Engineering* 1993; **110**:325–342.
36. Tezduyar T. Stabilization parameters and local length scales in SUPG and PSPG formulations. Proceedings of the *Fifth World Congress on Computational Mechanics*, Vienna, Austria, July 7–12, 2002, <http://wccm.tuwien.ac.at>.
37. Zienkiewicz OC, Zhu JZ. The Superconvergent patch recovery (SPR) and adaptive finite element refinement. *Computer Methods in Applied Mechanics and Engineering* 1992; **101**:207–224.
38. Wiberg NW, Abdulwahab F, Li XD. (1997). Error estimation and adaptive procedures based on superconvergent patch recovery. *Archives of Computer Methods in Engineering* 1997; **4**(3):203–242.
39. Ilinca F, Héty JF, Pelletier D. On stabilized finite element formulation for incompressible advective–diffusive transport and fluid flow problems. *Computer Methods in Applied Mechanics and Engineering* 2000; **188**: 235–257.
40. Chetverushkin BN. Kinetic schemes and their application for simulation of viscous gas dynamics problems. In *European Congress on Computational Methods in Applied Sciences and Engineering (ECCOMAS 2000)*, Oñate E *et al.* (eds), CIMNE: Barcelona 11–14 September, 2000.
41. Oñate E, Rojek J, Taylor RL, Zienkiewicz OC. Finite calculus formulation for analysis of incompressible solids using linear triangles and tetrahedra. *International Journal for Numerical Methods in Engineering* 2004; **59**:1473–1500.
42. Oñate E, Rojek J, Taylor RL, Zienkiewicz OC. Linear triangles and tetrahedra for incompressible problems using a finite calculus formulation. In *European Conference on Computational Mechanics (ECCM2001)*, Cracow, Poland, 26–29 June, 2001.
43. de Borst R. Simulation of strain localization: a reappraisal of the Cosserat continuum. *Continuum Computation* 1991; **8**:317–332.
44. Larsry D, Belytschko T. Localization limiters in transient problems. *International Journal of Solids and Structures* 1988; **24**:581–597.
45. Schreier HL, Chen Z. One dimensional softening with localization. *Journal of Applied Mechanics (ASME)* 1980; **53**:791–797.
46. de Borst R. Gradient-dependent plasticity: formulation and algorithmic aspects. *International Journal for Numerical Methods in Engineering* 1992; **35**:521–539.
47. Peric D, Yu J, Owen DRJ. On error estimates and adaptivity in elastoplastic solids: application to the numerical simulation of strain localization in classical and Cosserat continua. *International Journal for Numerical Methods in Engineering* 1994; **37**:1351–1379.
48. Borja R. Possibilities of the FIC method for strain localization problems. *Private communication*, 2001.